

Electronic Raman scattering in $\text{Cd}_{1-x}\text{Co}_x\text{Se}$

D. U. Bartholomew, E-K. Suh, A. K. Ramdas, and S. Rodriguez
Department of Physics, Purdue University, West Lafayette, Indiana 47907

U. Debska and J. K. Furdyna
Department of Physics, University of Notre Dame, Notre Dame, Indiana 46556
 (Received 22 July 1988)

The Raman spectrum of the diluted magnetic semiconductor $\text{Cd}_{1-x}\text{Co}_x\text{Se}$ ($x=0.035$ and 0.082) exhibits a line (ω_{PM}) associated with the transition between the Zeeman-split orbital Γ_2 ground-state levels of Co^{2+} and is characterized by $g=2.32$. Below 20 K, this Raman peak shifts to higher frequencies, signaling the onset of magnetic ordering. At low temperatures, spin-flip Raman scattering from electrons bound to shallow donors (ω_{SF}) is observed. The Raman shift as a function of magnetic field and temperature shows a large s - d exchange interaction ($\alpha N_0=320$ meV) and clear evidence of a bound magnetic polaron. Evidence of magnetic ordering at low temperatures, indicated by the temperature dependence of ω_{PM} , and the large antiferromagnetic temperature (T_{AF}) required to fit the temperature and magnetic-field dependence of ω_{SF} , indicate a significantly larger Co^{2+} - Co^{2+} antiferromagnetic coupling than is the case for Mn^{2+} - Mn^{2+} in, for example, $\text{Cd}_{1-x}\text{Mn}_x\text{Se}$.

I. INTRODUCTION

Diluted magnetic semiconductors (DMS's) are alloys in which the group-II atoms of a II-VI semiconductor are randomly replaced by magnetic atoms.^{1,2} DMS alloys with manganese as the magnetic substitute have been widely studied in recent years. Several phenomena have been traced to the presence of Mn^{2+} : for example, Raman electron paramagnetic resonance (EPR) of Mn^{2+} ions and magnetic phases due to antiferromagnetic coupling between Mn^{2+} ions have been observed. There also exists a strong sp - d exchange interaction between the localized spins of the d -like Mn^{2+} electrons and the spins of the s -like (p -like) conduction- (valence-) band electrons, which manifests itself in large effective g factors for the band electrons. This sp - d exchange interaction leads to large values for interband and exciton Zeeman splittings³ and the resultant giant Faraday effect,^{3,4} and spin-flip Raman scattering from donors.⁵ A systematic study of spin-flip Raman scattering in n -type DMS alloys containing manganese as the magnetic constituent can be found in Peterson *et al.*⁶

The atomic ground state of Mn^{2+} , ${}^6S_{5/2}$, in a tetrahedral crystal environment characteristic of, say, a zinc-blende structure undergoes a crystal-field splitting into a Γ_8 quadruplet and a Γ_7 doublet.⁷ Experimentally this crystal-field splitting is very small and can be ignored,⁸ allowing the ground state to be viewed as an orbital singlet with $S=\frac{5}{2}$. Recently, the interest in DMS alloys has extended to magnetic ions other than manganese. The atomic configuration of Fe^{2+} is $3d^6$ with a free-ion ground state of 5D_4 . Experimental observations on CdTe:Fe^{2+} (Ref. 9) have shown that the T_d crystal potential is much larger than the spin-orbit interaction; the 5D term splits into an orbital doublet (Γ_3) and higher-lying orbital triplet (Γ_5), each with $S=2$. Spin-orbit cou-

pling further splits the ${}^5\Gamma_3$ levels into $\Gamma_1+\Gamma_4+\Gamma_3+\Gamma_5+\Gamma_2$ with the nondegenerate, and hence nonmagnetic, Γ_1 as the ground state. Indeed, such a system will exhibit temperature-independent Van Vleck paramagnetism at low temperatures. Infrared magneto-absorption measurements on $\text{Hg}_{1-x}\text{Fe}_x\text{Te}$ show that Fe-based DMS alloys also have a large sp - d exchange interaction¹⁰ and indeed exhibit Van Vleck paramagnetism.

Another class of II-VI DMS alloys is based on Co^{2+} , which has a partially filled $3d^7$ -electron configuration. By virtue of Kramers's theorem, the odd number of electrons dictates that Co^{2+} must always exhibit ordinary paramagnetism. The magnetic behavior of Co^{2+} in a DMS alloy is determined by the nature of its ground state when introduced into the crystal. This arises from the splitting of the 28-fold-degenerate 4F term as a result of crystal-field and spin-orbit interaction and is discussed in Sec. III.

In this paper we present results on Raman scattering from n -type $\text{Cd}_{1-x}\text{Co}_x\text{Se}$ showing spin flip of magnetic ions and electrons bound to donors¹¹ and discuss them in the context of the above issues.

II. EXPERIMENTAL

The $\text{Cd}_{1-x}\text{Co}_x\text{Se}$ samples used in our investigations were single crystals grown by the modified vertical Bridgman method. This DMS system has a wurtzite structure and thus has a sixfold axis of crystal symmetry \hat{c} . The samples were not intentionally doped but were n type as a result of having "anonymous" donors. They were optically polished, using successively finer abrasives and polishing compounds, the final polish being accomplished with $0.05\ \mu\text{m}$ alumina powder. The samples had typical dimensions of $5\times 5\times 3\ \text{mm}^3$. The magnetic ion concentrations were determined by electron-microprobe analysis.

The Raman spectra were excited using the 6764- and 6471-Å lines of a Kr⁺-ion laser. Care was taken to prevent the incident laser beam from heating the samples; this was ensured by methodically decreasing the incident laser power until the position of the spin-flip feature was no longer affected. The scattered light was analyzed with a Spex double (and, when greater scattered light rejection was desired, a triple) monochromator and detected using standard photon-counting techniques.

The samples were cooled in a variable temperature optical cryostat¹² equipped with a superconducting coil capable of attaining magnetic fields of up to 60 kG. The temperature was monitored with a calibrated carbon-glass resistor located immediately above the sample and could be stabilized with a temperature controller over the range of 1.8–300 K.

Raman spectra were taken in the backscattering geometry, $\hat{k}_i \parallel \hat{k}_s$, where \hat{k}_i and \hat{k}_s are the incident and scattered wave vectors, respectively. Backscattering geometry was used in view of the strong absorption below the energy gap arising from intra-ion transitions of Co²⁺. The magnetic field was perpendicular to \hat{k}_i . Measurements were performed in either "parallel" ($\hat{\epsilon}_i \parallel \hat{\epsilon}_s$) or "crossed" ($\hat{\epsilon}_i \perp \hat{\epsilon}_s$) polarizations, where $\hat{\epsilon}_i$ and $\hat{\epsilon}_s$ are the polarizations of the incident and scattered electric fields, respectively.

III. RESULTS AND DISCUSSION

A. Co²⁺ spin flip

In Fig. 1 we show the Raman spectrum of Cd_{1-x}Co_xSe, $x = 0.035$, in a magnetic field (H) of 60 kG and at a temperature (T) of 60 K in which Stokes and anti-Stokes Raman peaks labeled "PM" (PM denotes paramagnetic) can be seen at 6.50 cm⁻¹. The PM peak shifts linearly with magnetic field and appears in the crossed polarization. Figure 2 displays the temperature dependence of ω_{PM} , the position of the PM peak, measured at 60 kG. Below ~ 20 K there is a distinct change of the PM position to higher Raman shifts, reaching 7.1 cm⁻¹ at 1.8 K. Figure 3 shows the linear magnetic-field dependence of ω_{PM} at 60 K and at 1.8 K. While the linear fit of the data for 60 K passes through the origin, that for 1.8 K suggests a finite Raman shift at 0 kG; in addition, the slope of ω_{PM} versus H increases by 7% upon cooling from 60 to 1.8 K. The PM peak for Cd_{1-x}Co_xSe, $x = 0.082$, shows a similar behavior, the shift of the peak being even larger than that for $x = 0.035$ as the temperature is lowered, having a value of 7.4 cm⁻¹ at 1.8 K. In addition, the PM peak for this sample was not observed with $H \parallel \hat{c}$.

We attribute the PM peak to Raman scattering between levels of the Zeeman-split ground state of the Co²⁺ ion, i.e., to the Raman EPR of Co²⁺. The magnitude of this splitting is given by

$$\hbar\omega_{PM} = g_{Co^{2+}}\mu_B H, \quad (1)$$

where $g_{Co^{2+}}$ is the Landé g factor for the Co²⁺ ions and μ_B is the Bohr magneton. From the above results, the g factor for CdSe:Co²⁺ is deduced to be 2.32 ± 0.04 . The

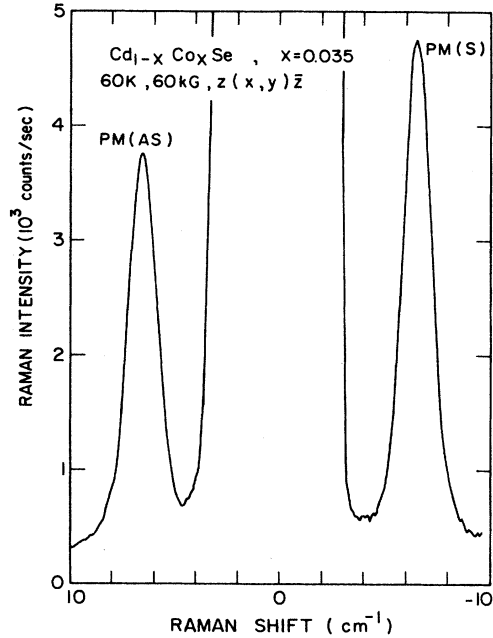


FIG. 1. Stokes (S) and anti-Stokes (AS) Raman lines labeled PM at ω_{PM} , resulting from $\Delta m_s = \pm 1$ spin-flip transitions within the Zeeman multiplet of Co²⁺ in Cd_{1-x}Co_xSe, $x = 0.035$. The wavelength of the exciting laser line is 6764 Å; the exciting power is 5 mW; the crystal orientation is $\hat{x} \parallel \hat{a} \parallel [2\bar{1}0]$, $\hat{y} \parallel \hat{c} \parallel [0001]$, and $\hat{z} \parallel \hat{b} \parallel [0\bar{1}10]$; the applied magnetic field $H = 60$ kG $\parallel \hat{c}$.

PM peak has previously been observed in Mn-based DMS alloys, yielding a g factor of 2.0 as expected for the ⁶S_{5/2} ground state of the manganese ion.¹³ Unlike Mn²⁺, the g factor for Co²⁺ in II-VI semiconductors varies from host

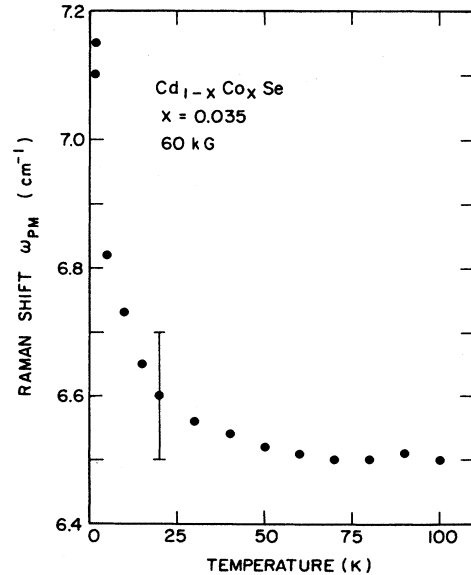


FIG. 2. Temperature dependence of the position of the PM peak, ω_{PM} , at a magnetic field of 60 kG for Cd_{1-x}Co_xSe, $x = 0.035$.

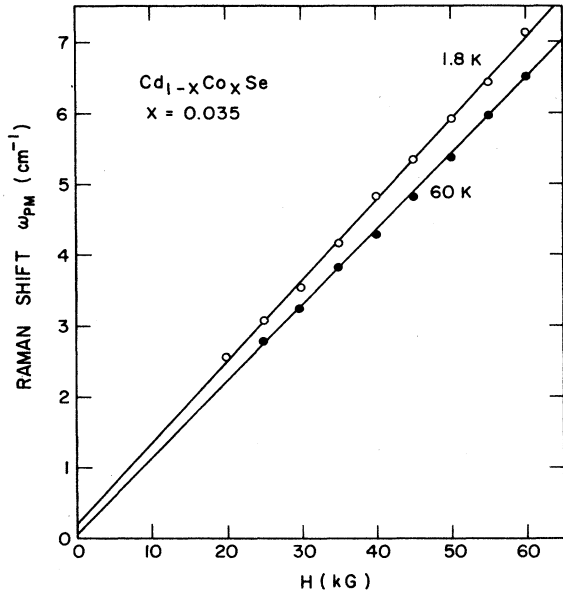


FIG. 3. Linear magnetic-field dependence of ω_{PM} for $\text{Cd}_{1-x}\text{Co}_x\text{Se}$, $x=0.035$, at 60 and 1.8 K. The lines are linear least-squares fits.

to host; for example, $g_{\text{Co}^{2+}}(\text{CdTe})=2.3093$ (Ref. 14), while $g_{\text{Co}^{2+}}(\text{ZnS})=2.248$ (Refs. 14 and 15). The excess of the g factor from the spin-only value of 2.00 is a result of the mixing of the higher-lying orbital states with the ground state by the spin-orbit coupling.

In order to discuss the nature of the g factor of Co^{2+} in $\text{Cd}_{1-x}\text{Co}_x\text{Se}$ we describe the 4F multiplet in the crystal potential. The site symmetry of Co^{2+} in a wurtzite (C_{6v}^4) crystal is C_{3v} . This reflects the tetrahedral coordination with its four nearest-neighbor Se atoms including a trigonal distortion along \hat{c} . The 4F multiplet splits into $^4\Gamma_1(C_{3v})$, two $^4\Gamma_2(C_{3v})$, and two $^4\Gamma_3(C_{3v})$ levels.⁷ Assuming that $^4\Gamma_2(C_{3v})$ is the lowest orbital state, symmetry considerations allow us to write the spin Hamiltonian as

$$\mathcal{H} = -\frac{6\lambda^2}{\Delta_1} \left[\frac{15}{4} - (\mathbf{S} \cdot \hat{c})^2 \right] + \mu_B \mathbf{H} \cdot \vec{g} \cdot \mathbf{S}, \quad (2)$$

where \vec{g} is a diagonal uniaxial tensor whose components are $g_{\parallel}=2$ and $g_{\perp}=2-(12\lambda/\Delta_1)$; Δ_1 is the energy separation between the lowest $^4\Gamma_2(C_{3v})$ and the doublet $^4\Gamma_3(C_{3v})$ corresponding to angular momentum along \hat{c} equal to ± 1 . Experimentally, contrary to these predictions, the g factor of Co^{2+} in $\text{Cd}_{1-x}\text{Co}_x\text{Se}$, $x=0.035$, is found to be isotropic and close to that found in $\text{ZnS}:\text{Co}^{2+}$ and $\text{CdTe}:\text{Co}^{2+}$. If the trigonal distortion is small and the largest components of the crystal field have T_d symmetry, the corresponding spin Hamiltonian for $^4\Gamma_2(T_d)$, assumed to be the lowest state, is

$$\mathcal{H} = g\mu_B \mathbf{S} \cdot \mathbf{H}, \quad (3)$$

where g is isotropic and given by $2-(8\lambda/\Delta_{52})$; now Δ_{52} defines the energy separation of $^4\Gamma_2(T_d)$ and $^4\Gamma_5(T_d)$. We

note that the small angular variation in the g factor of Co^{2+} in many II-VI host crystals, found by Ham *et al.*,¹⁴ is too small to have been observed in our experiments. Admixture of the 4F states with higher excited multiplets (e.g., 4P) has also been disregarded in this model.¹⁶ The ground-state orbital singlet $^4\Gamma_2(T_d)$ becomes $\Gamma_8(T_d)$ when the spin is taken into account. The small trigonal distortion splits this level into the two Kramers doublets $\Gamma_4(C_{3v})$ and $\Gamma_{5+6}(C_{3v})$ corresponding to $m_s = \pm \frac{1}{2}$ and $\pm \frac{3}{2}$, respectively. Their energy separation, $2D$, was found to be 1.34 cm^{-1} in $\text{CdS}:\text{Co}^{2+}$ with $\Gamma_4(C_{3v})$ being the lower.¹⁷

The g factor in $\text{Cd}_{1-x}\text{Co}_x\text{Se}$ was found to increase slightly with decreasing temperature. From the data in Fig. 3, for $x=0.035$, we deduce an increase in the g factor from 2.29 ± 0.03 at 60 K to 2.46 ± 0.04 at 1.8 K. A nearly identical trend was seen for $x=0.082$. This suggests that λ/Δ_{52} is temperature dependent or, alternately, affected by short-range magnetic ordering between the Co^{2+} ions as discussed below.

The increase in the ω_{PM} at low temperatures, as seen in Fig. 2, may also be explained as a thermal population effect. For $g_{\text{Co}^{2+}}\mu_B H > 2|D|$,¹⁸ three PM Stokes peaks should be present with frequency shifts of $g_{\text{Co}^{2+}}\mu_B H - 2D$ for $|-\frac{3}{2}\rangle \rightarrow |-\frac{1}{2}\rangle$, $g_{\text{Co}^{2+}}\mu_B H$ for $|-\frac{1}{2}\rangle \rightarrow |+\frac{1}{2}\rangle$, and $g_{\text{Co}^{2+}}\mu_B H + 2D$ for $|+\frac{1}{2}\rangle \rightarrow |+\frac{3}{2}\rangle$. For high temperatures, with $k_B T > g_{\text{Co}^{2+}}\mu_B H$, one should see three peaks (or a single broad peak if they are not resolved) centered at $g_{\text{Co}^{2+}}\mu_B H$. As the temperature is decreased, the relative intensities of these three PM peaks will change. Ultimately, only the $|-\frac{3}{2}\rangle$ -spin sublevel will be populated and the PM peak at $g_{\text{Co}^{2+}}\mu_B H - 2D$ will dominate the spectrum. Through a similar argument, the nonzero intercept for ω_{PM} at 1.8 K seen in Fig. 3 would represent $2D$. The $|\pm \frac{3}{2}\rangle$ sublevels should be the ground state at $H=0$ (the sign of D should be negative) for this effect to explain the trends shown in Figs. 2 and 3. This is unlikely since the $|\pm \frac{1}{2}\rangle$ sublevels are the ground state at $H=0$ in $\text{CdS}:\text{Co}^{2+}$, which closely resembles $\text{CdSe}:\text{Co}^{2+}$.¹⁷ Finally, our measurements were unable to resolve three PM peaks which implies that $2D$ is smaller than the spectrometer resolution of 0.6 cm^{-1} .

The increase in the PM Raman shift at low temperatures, as seen in Fig. 2, and the nonzero intercept for ω_{PM} at 1.8 K, seen in Fig. 3, is similar to that seen in Mn-based DMS's and could indicate the approach of a paramagnetic to spin-glass phase transition. That is, the PM peak continuously evolves into the high-frequency component of the one-magnon excitation which has been split by the magnetic field (M_+).¹³ Extrapolation of the linear magnetic-field dependence of the PM peak at 1.8 K for the two samples suggests a magnon frequency of $0.18 \pm 0.02 \text{ cm}^{-1}$ for $x=0.035$ and $0.60 \pm 0.26 \text{ cm}^{-1}$ for $x=0.082$. This strongly suggests that the increase in the PM position at low temperatures is due to the formation of a magnon and is not solely due to the increase in the g factor of the Co^{2+} ion. The increase in the magnon frequency with increasing x has been observed in Mn-based DMS's. It is consistent with the notion that antiferro-

magnetic clusters are present in DMS alloys, their size increasing with x ; this will create an increased "effective-exchange" field between adjacent Co^{2+} moments, leading to a larger magnon frequency.¹⁹

Finally, the resonant enhancement of the PM peak when the incident photon energy approaches that of the band gap suggests a Raman mechanism involving inter-band transitions in conjunction with a mutual flip of a band electron spin and a Co^{2+} spin via the sp - d exchange interaction, as has been invoked to describe similar behavior for the Raman EPR of Mn^{2+} in Mn-based DMS alloys.¹³

B. Donor spin flip

Figure 4 shows a Raman peak labeled SF (SF denotes spin flip) for $\text{Cd}_{1-x}\text{Co}_x\text{Se}$, $x=0.035$, which exhibits higher Raman shifts with increasing applied magnetic field. Figure 5 shows its position (ω_{SF}) at various temperatures as a function of the magnetic field \mathbf{H} along \hat{c} . The intensity of SF decreased with increasing temperature and the peak disappeared for $T > 80$ K. Experimentally it was found that SF for a given magnetic field occurs at the same position for $\mathbf{H} \parallel \hat{c}$ and $\mathbf{H} \perp \hat{c}$. These features, characteristic of spin-flip Raman scattering from electrons bound to donors, are clearly seen in Fig. 5: large Raman shifts at moderate magnetic fields, becoming even larger as the temperature is decreased, evidence of saturation of ω_{SF} at high magnetic fields and low temperatures, and an indication of a finite Raman shift at zero magnetic field at approximately 2.5 cm^{-1} .

Figure 6 shows a set of spin-flip Raman data for $\text{Cd}_{1-x}\text{Co}_x\text{Se}$, $x=0.082$, at 1.8 and 10 K with either $\mathbf{H} \parallel \hat{c}$ or $\mathbf{H} \perp \hat{c}$. As can be seen, ω_{SF} in this sample exhibits anisotropy as the orientation of \mathbf{H} is changed; the anisotropy was present at all temperatures for which the SF peak was observed. The inset in Fig. 6 shows the variation of ω_{SF} with angle θ between \mathbf{H} and \hat{c} ; the dashed curve is $\sin^2\theta$ fitted to pass through $\omega_{\text{SF}}(\theta=0^\circ)$ and $\omega_{\text{SF}}(\theta=90^\circ)$.

The large g factors, deduced from the linear regions of Figs. 5 and 6, are due to the presence of the exchange interaction between the spins of the s -like conduction

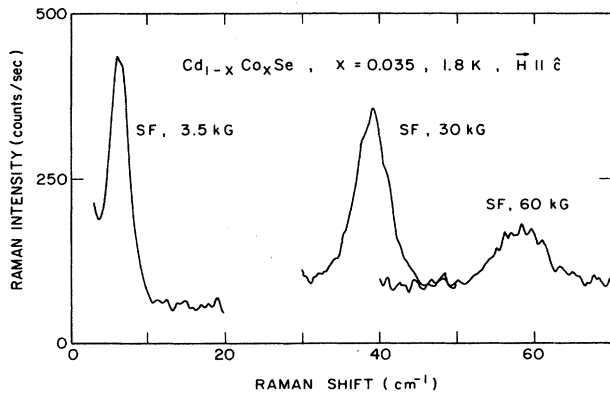


FIG. 4. Raman spectra of $\text{Cd}_{1-x}\text{Co}_x\text{Se}$, $x=0.035$, showing the spin flip of electrons bound to donors (SF) for three values of magnetic field ($\mathbf{H} \parallel \hat{c}$).

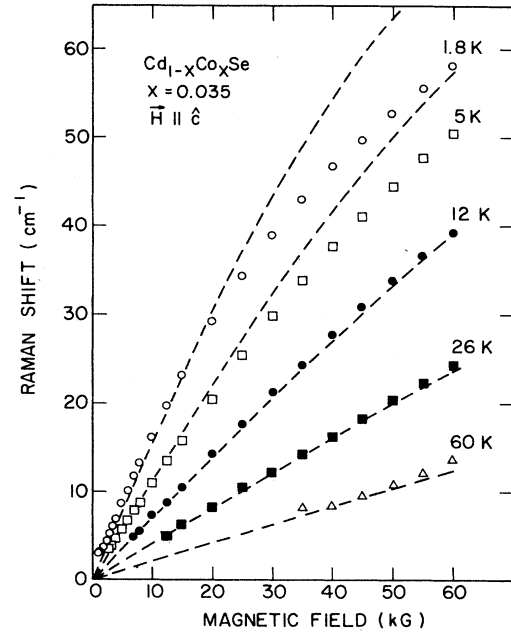


FIG. 5. Magnetic-field and temperature dependence of the Raman shift associated with the spin flip of electrons bound to donors in $\text{Cd}_{1-x}\text{Co}_x\text{Se}$, $x=0.035$, with $\mathbf{H} \parallel \hat{c}$. The theoretical curves result from Eqs. (3) and (4) with $\bar{x}\alpha N_0=7.78 \text{ meV}$ and $T_{\text{AF}}=5.91 \text{ K}$. Note that the experimental data have a finite intercept at $H=0$ and $T=1.8 \text{ K}$ at $\sim 2.5 \text{ cm}^{-1}$, indicating the presence of a bound magnetic polaron.

(donor) electrons and those of the d -like Co^{2+} electrons, the so-called " s - d " exchange interaction. The s - d exchange coupling can be approximated by a Heisenberg interaction. The magnetic portion of the Hamiltonian for the donor has the form

$$\mathcal{H}_M(\mathbf{S}_i, \mathbf{s}) = -\alpha N_0 \sum_i \mathbf{S}_i \cdot \mathbf{s} + g^* \mu_B \mathbf{H} \cdot \mathbf{s}, \quad (4)$$

where α is the exchange integral between the localized Co^{2+} spins (\mathbf{S}_i) and that of the donor electron (\mathbf{s}), N_0 is the number of cations per unit volume, and g^* is the intrinsic g factor of conduction electrons, taken to be 0.52 for CdSe.⁶ The second term describes the intrinsic Zeeman splitting of the conduction band. The first term yields an additional Zeeman splitting at $\mathbf{k}=0$ of $6A$, where

$$6A = \alpha \frac{M}{g_{\text{Co}^{2+}} \mu_B}, \quad (5)$$

and M is the magnetization of the Co^{2+} ions.²⁰ For small x and assuming $2D$ is small, the magnetization can be approximated by a Brillouin-like function B_S ,²¹

$$M = g_{\text{Co}^{2+}} \mu_B \bar{x} N_0 S_B S \left[\frac{g_{\text{Co}^{2+}} \mu_B H}{k_B (T + T_{\text{AF}})} \right], \quad (6)$$

where \bar{x} and T_{AF} (AF denotes antiferromagnetic) are empirical constants introduced in order to take into ac-

count small amounts of antiferromagnetic coupling between the Co^{2+} ions, and $S = \frac{3}{2}$ for Co-based DMS alloys.

In the mean-field approximation, we neglect the finite Raman shift at zero field, the so-called bound magnetic polaron (BMP), and consider only those portions of the spin-flip Raman shift data which are linear in H . The effective g factor is given by²²

$$g_{\text{eff}} = \frac{5\bar{x}(\alpha N_0)}{4k_B(T + T_{\text{AF}})} g_{\text{Co}^{2+}} + g^* = g_x + g^* \quad (7)$$

In Fig. 7 we show a plot of g_x^{-1} versus T for the two $\text{Cd}_{1-x}\text{Co}_x\text{Se}$ samples. The results for $T < 40$ K are fitted with a linear least-squares fit,²³ yielding $T_{\text{AF}} = 5.91$ K, $\bar{x}\alpha N_0 = 7.78$ meV for $x = 0.035$ and $T_{\text{AF}} = 13.01$ K, $\bar{x}\alpha N_0 = 11.7$ meV for $x = 0.082$ with $\vec{H} \perp \hat{c}$; the dashed lines in Figs. 5 and 6 are theoretical curves of ω_{SF} versus H based on Eqs. (5) and (6) and these parameters. It is interesting to note that for $x = 0.035$ the curves deviate significantly for high magnetic fields at 5 and 1.8 K. However, a fit of the experimental data for $x = 0.035$, specifically for 5 and 1.8 K, yields $\bar{x}\alpha N_0 = 6.7$ meV, $T_{\text{AF}} = 3.87$ K and $\bar{x}\alpha N_0 = 5.44$ meV, $T_{\text{AF}} = 3.54$ K, respectively; the fits to the data at these two temperatures

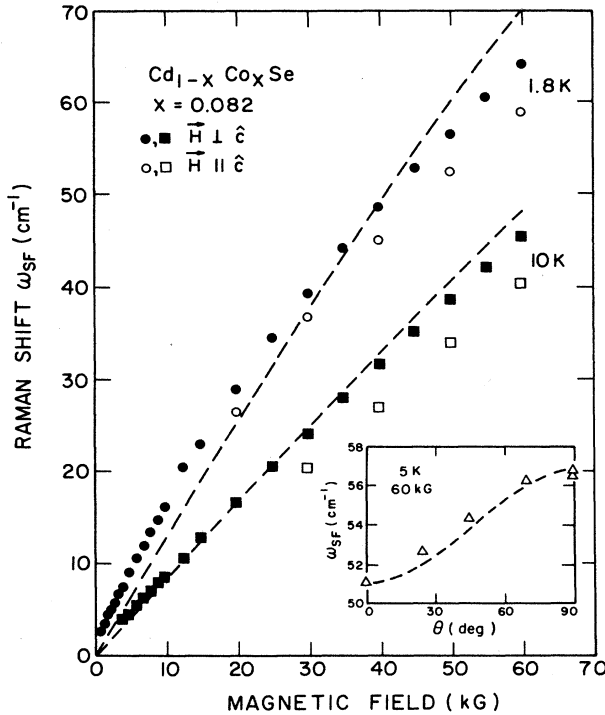


FIG. 6. Magnetic-field and temperature dependence of the peak spin-flip Raman shift (SF) associated with the spin flip of electrons bound to donors in $\text{Cd}_{1-x}\text{Co}_x\text{Se}$, $x = 0.082$, with either $\vec{H} \parallel \hat{c}$ or $\vec{H} \perp \hat{c}$. The theoretical curves for $\vec{H} \perp \hat{c}$ result from Eqs. (3) and (4) with $\bar{x}\alpha N_0 = 11.7$ meV and $T_{\text{AF}} = 13.0$ K. The inset shows the dependence of SF on the angle θ between \vec{H} and \hat{c} ; the dashed line is $\sin^2\theta$ fitted to pass through $\omega_{\text{SF}}(\theta=0^\circ)$ and $\omega_{\text{SF}}(\theta=90^\circ)$.

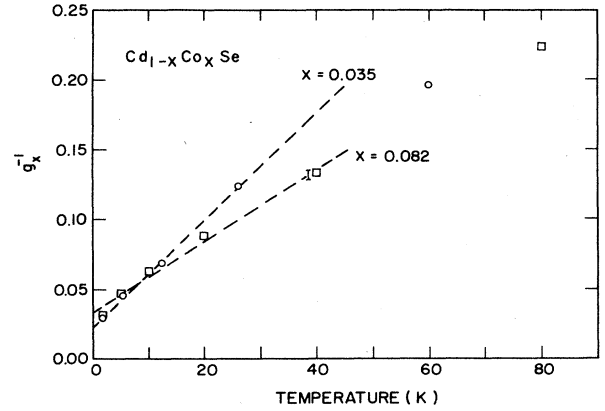


FIG. 7. The inverse g factor (g_x^{-1}) vs temperature in the $\text{Cd}_{1-x}\text{Co}_x\text{Se}$ samples. The straight lines are fits to the experimental data for $T \leq 40$ K.

are then significantly better. The theoretical curves for $x = 0.082$ (the dashed curves in Fig. 6) also deviate somewhat for 1.8 K, although the departure is not as dramatic as for $x = 0.035$. The origin of these effects is not clear. However, it is not unexpected, given the phenomenological character of Eq. (6).

We note here that the values for T_{AF} in $\text{Cd}_{1-x}\text{Mn}_x\text{Se}$ are 1.38 K for $x = 0.051$ and 2.28 K for $x = 0.104$. The values for T_{AF} in $\text{Cd}_{1-x}\text{Co}_x\text{Se}$ for comparable values of x appear to be at least 5 times greater than those in $\text{Cd}_{1-x}\text{Mn}_x\text{Se}$. Although T_{AF} is a phenomenological constant, it reflects approximately the strength of the exchange interactions between Co^{2+} spins including more distant neighbors.²⁴ Thus it appears that such exchange interactions are stronger for Co^{2+} ions than those for Mn^{2+} ions in CdSe.

It is clear that the variation of \bar{x} with x in $\text{Cd}_{1-x}\text{Co}_x\text{Se}$ has to be known in order to deduce αN_0 from $\bar{x}\alpha N_0$. Shapira *et al.*²⁵ have derived expressions for the x dependence of \bar{x}/x for Mn-based DMS alloys considering the probability that a Mn^{2+} ion belongs to one of several types of clusters: viz., isolated singlets (P_1), pairs (P_2), open triplets (P_3), or closed triplets (P_4); their expression fits known values of \bar{x}/x very closely for $x \leq 0.10$. Equation (8) from Ref. 22, after a slight modification for Co^{2+} having a total spin of $\frac{3}{2}$, yields²⁶

$$\bar{x}/x = (P_1 + P_3/3 + P_4/9) + [(1 - P_1 - P_2 - P_3 - P_4)/5] \quad (8)$$

Equation (8) yields $\bar{x}/x = 0.69$ for $x = 0.035$ and $\bar{x}/x = 0.46$ for $x = 0.082$. With this, the s - d exchange constant αN_0 is estimated to be 322 meV for $x = 0.035$ and 318 meV for $x = 0.082$ with $\vec{H} \perp \hat{c}$. For comparison, we note $\alpha N_0 = 261$ meV for $\text{Cd}_{1-x}\text{Mn}_x\text{Se}$.²⁷

The origin of the anisotropy in the spin flip versus \vec{H} plot for $\text{Cd}_{1-x}\text{Co}_x\text{Se}$, $x = 0.082$, seen in Fig. 6, is not clear. It cannot be attributed to any spatial variation of x within the sample; the spin-flip peak position at 5 K and

60 kG varied by 0.5 cm^{-1} over the surface of the sample, suggesting a variation in x of only 1%. It is worthwhile to note that anisotropy of this type has not been observed in $\text{Cd}_{1-x}\text{Mn}_x\text{Se}$ or $\text{Cd}_{1-x}\text{Mn}_x\text{S}$.²⁸ Referring to Eq. (5), the observed anisotropy could arise if αN_0 , $g_{\text{Co}^{2+}}$, or M depends upon the angle θ between \mathbf{H} and $\hat{\mathbf{c}}$. The exchange interaction α is not expected to show any dependence on θ due to the symmetric nature of the s -like conduction-band wave functions.²⁹ The g factor for Co^{2+} is expected to vary with θ , although for $\text{CdS}:\text{Co}^{2+}$ this variation is only 1% between $\mathbf{H}\perp\hat{\mathbf{c}}$ and $\mathbf{H}\parallel\hat{\mathbf{c}}$;¹⁷ this is much smaller than the $\sim 10\%$ variation for SF shown in Fig. 6.

Anisotropy of the magnetic susceptibility ($\chi=M/H$) in $\text{Zn}_{1-x}\text{Co}_x\text{O}$, $x=0.00034$, has been observed by Brumage;³⁰ this anisotropy increased with decreasing temperature, varying from 1.3×10^{-7} cgs emu at 23 K to 24.2×10^{-7} cgs emu at 4.2 K, where $\chi_{\perp}(\theta=90^\circ)$ exceeds $\chi_{\parallel}(\theta=0^\circ)$. Both CdSe and ZnO have wurtzite structure. Thus, we expect the magnetization of Co^{2+} in CdSe (and, hence, SF) to display some anisotropy. The anisotropy of SF in $\text{Cd}_{1-x}\text{Co}_x\text{Se}$, $x=0.082$, is constant between 1.8 and 20 K, but decreases slightly for 40 K; this insensitivity for $T < 20$ K may be due to the large effective temperature $T + T_{\text{AF}}$, where $T_{\text{AF}}=13.1$ K. Like $\text{ZnO}:\text{Co}^{2+}$, Fig. 6 suggests that, for $\text{CdSe}:\text{Co}^{2+}$, $\chi_{\perp} > \chi_{\parallel}$. Brumage also states that the susceptibility should vary as $\sin^2\theta$ between χ_{\parallel} and χ_{\perp} . The inset of Fig. 6 indicates that this dependence is true for $\text{Cd}_{1-x}\text{Co}_x\text{Se}$, $x=0.082$, although we note that, for 5 K and 60 kG, SF (and, hence, the magnetization) displays a slight saturation. It is unclear why no anisotropy was observed for SF in $\text{Cd}_{1-x}\text{Co}_x\text{Se}$, $x=0.035$. Preliminary measurements on a sample with a nominal Co^{2+} concentration of $x=0.06$ also show a degree of SF anisotropy intermediate to the previous two samples. We plan to study a variety of additional $\text{Cd}_{1-x}\text{Co}_x\text{Se}$ samples in order to determine whether this behavior is due to some accidental characteristics of the sample.

In order to discuss the experiential results on the bound magnetic polaron, we use the theory of Dietl and Spaček³¹ reviewed in Ref. 6. According to this theory the magnetic-field-dependent peak position of the spin-flip Raman line, $\bar{\Delta}$, satisfies

$$\bar{\Delta}^2 \mp 2\epsilon_p \bar{\Delta} - \bar{\Delta} \Delta_0 \coth \left[\frac{\bar{\Delta} \Delta_0}{4\epsilon_p k_B T} \right] - 4\epsilon_p k_B T = 0, \quad (9)$$

where \mp refers to the Stokes and anti-Stokes components, ϵ_p is the characteristic BMP energy for an s -like wave function with an effective Bohr radius of a , $\Delta_0 = g_x \mu_B H + g^* \mu_B H$ [in the mean-field approximation of Eq. (7)], and

$$\epsilon_p = \frac{W_0^2}{4k_B(T + T_{\text{AF}})}, \quad (10)$$

where, in the notation of Heiman *et al.*,²²

$$W_0^2 = \frac{5}{32} \frac{\bar{x}(\alpha N_0)^2}{\pi a^3 N_0}. \quad (11)$$

Using Eq. (9) to fit the low-magnetic-field SF data yields $T_{\text{AF}}=5.62$ K, $\bar{x}\alpha N_0=7.69$ meV, and $W_0=0.143$ meV for $x=0.035$, and $T_{\text{AF}}=10.6$ K, $\bar{x}\alpha N_0=10.07$ meV, and $W_0=0.532$ meV for $x=0.082$ ($\mathbf{H}\perp\hat{\mathbf{c}}$). For $x=0.035$ the values for T_{AF} and $\bar{x}\alpha N_0$ are in good agreement with those deduced earlier in the paper ignoring BMP effects, whereas those for $x=0.082$ are somewhat smaller. The adjustable parameter W_0 is a measure of the effective Bohr radius, which can be compared with 43.1 \AA for CdSe.⁶ Using Eq. (11) and assuming $N_0=N_0(\text{CdSe})=1.78 \times 10^{22} \text{ cm}^{-3}$,³² a is 69 \AA for $x=0.035$ and 30 \AA for $x=0.082$. The Bohr radius for $x=0.082$ is consistent with the notion that the formation of the bound magnetic polaron causes the orbit of the localized donor electron to shrink. The origin of the large a for $x=0.035$ is the small value of W_0 and implies a peak position of the BMP of 1.5 cm^{-1} , which is smaller than that observed. From Fig. 5, the position of the BMP peak is about 2.5 cm^{-1} at 1.8 K, which yields $W_0=0.370$ meV and $a=37 \text{ \AA}$, this Bohr radius shows the expected trend, viz, a decreases with increasing magnetic susceptibility.

As discussed in the preceding section, both of the $\text{Cd}_{1-x}\text{Co}_x\text{Se}$ samples that were studied showed evidence that a paramagnetic to spin-glass magnetic phase transition is being approached as the temperature decreases in the range of $T < 10$ K. The theory for the BMP developed by Dietl and Spaček is valid for x well below the onset of any magnetic freezing, where the magnetization can be well characterized. Thus, the above BMP analysis should be viewed with due reservations.

IV. CONCLUSIONS

The measurements reported in this paper have shown spin-flip Raman scattering from Co^{2+} ions in $\text{Cd}_{1-x}\text{Co}_x\text{Se}$ yielding a g factor of 2.32. The g factor displayed no anisotropy with the direction of the magnetic field with respect to the c axis; the expected anisotropy is too small for these measurements to detect. Even for x as small as 0.035, ω_{PM} shifts to higher frequencies for temperatures less than 20 K, a behavior characteristic of PM evolving into the high-frequency component of a magnon in a magnetic field; this is indicative of the presence of magnetically ordered clusters of Co^{2+} spins. A comparison of similar behavior observed in $\text{Cd}_{1-x}\text{Mn}_x\text{Te}$ indicates that the $\text{Co}^{2+}\text{-Co}^{2+}$ exchange interaction is larger than the $\text{Mn}^{2+}\text{-Mn}^{2+}$ exchange interaction in Mn-based DMS alloys.

Spin-flip Raman scattering from electrons bound to donors observed in this investigation demonstrates the existence of a large s - d exchange coupling between the spins of the donor electrons and those of the Co^{2+} ions, with $\alpha N_0=320$ meV, 23% larger than that found in $\text{Cd}_{1-x}\text{Mn}_x\text{Se}$. The bound magnetic polaron appears at $\sim 2.5 \text{ cm}^{-1}$, which is smaller than its position of $\sim 7 \text{ cm}^{-1}$ in $\text{Cd}_{1-x}\text{Mn}_x\text{Se}$; the origin of this smaller BMP is the total spin of $\frac{3}{2}$ for Co^{2+} (as opposed to total spin of $\frac{5}{2}$ for Mn^{2+}) as well as the large effective temperature

$T + T_{AF}$ found in Co-based DMS alloys. The values of T_{AF} are found to be 5 times larger than those found in $\text{Cd}_{1-x}\text{Mn}_x\text{Se}$ having equivalent x ; this indicates a larger interion exchange interaction between Co^{2+} ions. This result is in qualitative agreement with the magnetic-susceptibility measurements of Lewicki *et al.*³³ on $\text{Cd}_{1-x}\text{Co}_x\text{Se}$, which indicate a nearest-neighbor (NN) exchange constant $J_{NN}/k_B \sim 40$ K. The ω_{SF} data for high H and $T > 5$ K can be adequately described using mean-field theory, although for lower temperatures the effects of magnetic ordering need to be taken into account. Based on magnetic-susceptibility anisotropy in $\text{ZnO}:\text{Co}^{2+}$, one expects (at least in principle) to observe some anisotropy in effects involving the s - d exchange

processes in $\text{Cd}_{1-x}\text{Co}_x\text{Se}$; such effects were seen for $x = 0.082$, but not for $x = 0.035$.

ACKNOWLEDGMENTS

We thank Dr. A. Lewicki and Professor W. H. Brumage for useful discussions. The work reported in this paper received support from the U.S. National Science Foundation under Grant No. DMR-85-20866 and from the Defense Advanced Research Projects Agency-University Research Initiative Consortium "Diluted Magnetic Semiconductors and their Heterostructures" administered by the U.S. Office of Naval Research (Contract No. N00014-86-K-0760).

- ¹J. K. Furdyna, *J. Appl. Phys.* **53**, 7637 (1982).
- ²A. K. Ramdas, *J. Appl. Phys.* **53**, 7649 (1982).
- ³J. A. Gaj, R. R. Gałazka, and M. Nawrocki, *Solid State Commun.* **25**, 193 (1978).
- ⁴D. U. Bartholomew, J. K. Furdyna, and A. K. Ramdas, *Phys. Rev. B* **34**, 6943 (1986).
- ⁵F. F. Geyer and H. Y. Fan, *IEEE J. Quantum Electron.* **QE-16**, 1365 (1980); M. Nawrocki, R. Planel, G. Fishman, and R. R. Gałazka, *Phys. Rev. Lett.* **46**, 735 (1981).
- ⁶D. L. Peterson, D. U. Bartholomew, U. Debska, A. K. Ramdas, and S. Rodriguez, *Phys. Rev. B* **32**, 323 (1985).
- ⁷The group-theoretical notation for the irreducible representations follows G. F. Koster, J. O. Dimmock, R. G. Wheeler, and H. Statz, *Properties of the Thirty-two Point Groups* (MIT Press, Cambridge, MA, 1966).
- ⁸J. Lambe and C. Kikuchi, *Phys. Rev.* **119**, 1256 (1960).
- ⁹G. A. Slack, S. Roberts, and J. T. Vallin, *Phys. Rev. B* **187**, 511 (1969).
- ¹⁰H. Serre, G. Bastard, C. Rigaux, J. Mycielski, and J. K. Furdyna, in *Proceedings of the 4th International Conference on the Physics of Narrow-Gap Semiconductors, Linz, 1982*, edited by E. Gornik, H. Heinrich, and L. Palmethofer (Springer, New York, 1982), p. 321.
- ¹¹A preliminary report of these results was presented by E.-K., Suh, D. U. Bartholomew, J. K. Furdyna, U. Debska, A. K. Ramdas, and S. Rodriguez, *Bull. Am. Phys. Soc.* **32**, 802 (1987).
- ¹²Model 10 DT "Super-Varitemp" Optical Magnetic Cryostat, Janis Research Co., Wilmington, MA 01887; the superconducting coil was manufactured by American Magnetics, Inc., Oak Ridge, TN 37830.
- ¹³A. Petrou, D. L. Peterson, S. Venugopalan, R. R. Gałazka, A. K. Ramdas, and S. Rodriguez, *Phys. Rev. B* **27**, 3471 (1983).
- ¹⁴F. S. Ham, G. W. Ludwig, G. D. Watkins, and H. H. Woodbury, *Phys. Rev. Lett.* **5**, 468 (1960).
- ¹⁵Our Raman-EPR measurements performed on $\text{Zn}_{0.999}\text{Co}_{0.001}\text{S}$ (unpublished) also yielded $g = 2.25$.
- ¹⁶A. Abragam and B. Bleaney, *Electron Paramagnetic Resonance in Transition Ions* (Clarendon, Oxford, 1970), pp. 742-760.
- ¹⁷K. Morigaki, *J. Phys. Soc. Jpn.* **19**, 2064 (1964).
- ¹⁸This condition is met for a field of 60 kG since $2D$, as determined by electron-spin resonance of Co^{2+} in CdSe, is $1.54 \pm 0.03 \text{ cm}^{-1}$; see Teruhiko Hoshina, *J. Phys. Soc. Jpn.* **21**, 1608 (1966). This value is comparable with that in $\text{CdS}:\text{Co}^{2+}$ (1.34 cm^{-1}) which is surprising since $2D$ is related to the departure of c/a from its ideal value of $\sqrt{8/3}$, which is smaller for CdSe than for CdS.
- ¹⁹S. Venugopalan, A. Petrou, R. R. Gałazka, A. K. Ramdas, and S. Rodriguez, *Phys. Rev. B* **25**, 2681 (1982).
- ²⁰G. Bastard, C. Rigaux, and A. Mycielski, *Phys. Status Solidi B* **79**, 585 (1977); J. A. Gaj, J. Ginter, and R. R. Gałazka, *ibid.* **89**, 655 (1978).
- ²¹J. A. Gaj, R. Planel, and G. Fishman, *Solid State Commun.* **29**, 435 (1979). We follow the notation for B_S used in F. Reif, *Fundamentals of Statistical and Thermal Physics* (McGraw-Hill, New York, 1965), p. 259.
- ²²D. Heiman, P. A. Wolff, and J. Warnock, *Phys. Rev. B* **27**, 4848 (1983).
- ²³Spin-flip measurements on $\text{Cd}_{1-x}\text{Mn}_x\text{Se}$ have indicated that either $\bar{\chi}$ or T_{AF} or both show a temperature dependence for $T > 40$ K; see Ref. 6.
- ²⁴G. Barilero, C. Rigaux, N. H. Hau, J. C. Picoche, and W. Giriat, *Solid State Commun.* **62**, 345 (1987).
- ²⁵Y. Shapira, S. Foner, D. H. Ridgley, K. Dwight, and A. Wold, *Phys. Rev. B* **30**, 4021 (1984).
- ²⁶The term $P_4/15$ in Eq. (8) of Ref. 22 becomes $P_4/9$ in the case of Co-based DMS alloys.
- ²⁷Y. Shapira, D. Heiman, and S. Foner, *Solid State Commun.* **44**, 1243 (1982).
- ²⁸D. U. Bartholomew *et al.* (unpublished).
- ²⁹R. L. Aggarwal, S. N. Jasperson, J. Stankiewicz, Y. Shapira, S. Foner, B. Khazai, and A. Wold, *Phys. Rev. B* **28**, 6907 (1983).
- ³⁰W. H. Brumage, Ph.D. Thesis, University of Oklahoma, 1964 (unpublished). Note the units for χ used for the data are cm^3 per g of sample; the anisotropy is $\Delta\chi = \chi_{\perp} - \chi_{\parallel}$.
- ³¹T. Dietl and J. Spałek, *Phys. Rev. Lett.* **48**, 355 (1982); see also *Phys. Rev. B* **28**, 1548 (1983).
- ³²The intercation distance in CdSe is taken to be 4.296 \AA ; see, for example, D. R. Yoder-Short, U. Debska, and J. K. Furdyna, *J. Appl. Phys.* **58**, 4056 (1985).
- ³³A. Lewicki, A. I. Schindler, and J. K. Furdyna (private communication).